ChemComm

Accepted Manuscript

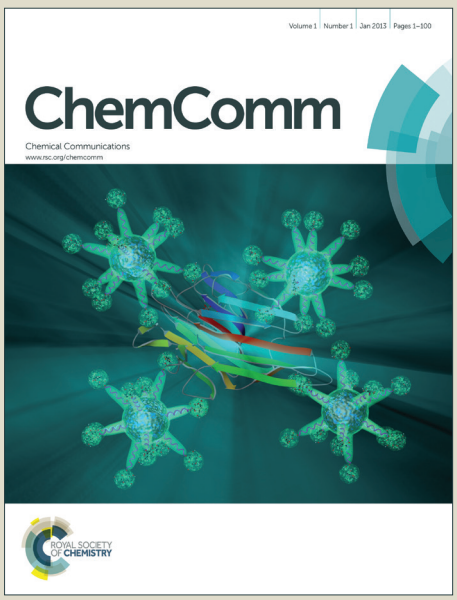

ROYAL SOCIETY OF CHEMISTRY

www.rsc.org/chemcomm

ChemComm

RSCPublishing

COMMUNICATION

Temperature-responsive DNA-gated nanocarriers for intracellular controlled release†

Cite this: DOI: 10.1039/x0xx00000x

Zhengze Yu,‡ Na Li,‡ Peipei Zheng, Wei Pan and Bo Tang*

Received 00th January 2014,
Accepted 00th January 2014

DOI: 10.1039/x0xx00000x

www.rsc.org/chemcomm

We report a novel strategy to construct temperature-responsive nanocarriers for controlled release based on mesoporous silica and reversible single-stranded DNA valves.

The development of nanocarriers as drug delivery platforms has emerged as one of the most innovative biomedical applications over the past decade.[1] Recently, much attention has been paid to develop stimuli-triggered nanocarriers that can regulate the release of the cargo effectively in response to a given stimulus relying on pH change,[2] enzymatic activity,[3] redox activation,[4] competitive binding,[5] photoirradiation[6] and temperature change.[7] Among these approaches, temperature-responsive drug delivery holds great promise because the local body temperature can change with ambient conditions and diseases in some cases.[8] As a potential candidate, DNA-based gatekeeper provides new possibilities for controlled drug delivery due to the easy synthesis and programmability, good biocompatibility and high cellular uptake. Many efforts have been made to exploit DNA-gated nanocarriers for controlled release upon exposure to the specific stimulus.[9] Most of these platforms performed well in opening the valve to release the cargo molecules. However, there is no report for the body temperature-triggered DNA-gated nanocarrier, in which the cargo molecules can be released controllably at body temperature. Thus, it is highly imperative to develop an on-command delivery system that the valve can be opened and closed in the range of body temperature, which could release the cargo molecules precisely and avoid unexpected release.

Here we present a simple and effective strategy to construct temperature-responsive nanocarrier, in which the cargo molecules can be loaded into the mesoporous silica pores and then coated with reversible single-stranded DNA valves. The DNA-gated nanocarrier can release the guests controllably at different temperature without any external stimulus and the critical release temperature of the nanocarrier can be turned by changing the length of single-stranded DNA oligonucleotides. Mesoporous silica nanoparticles (MSNs) were selected as the scaffold of the nanocarrier because of their high surface area, large pore volume, tunable pore size, easy functionalization and good biocompatibility.[10] When carboxyl modified single-stranded DNA was anchored with amino group on the surface of MSNs acting as the valve, the pre-loaded cargo could be released in a controlled manner. As the DNA was negatively charged while MS-NH_2 was positively charged, the DNA valves can absorb on the surface of the silica shell via electrostatic interaction, resulting in the "off" state.[11] When the temperature increased, the weak electrostatic interaction between mesoporous silica and DNA was destroyed, leading to the "on" state of the valves and the release of the cargo molecules from the nanocarrier. While the temperature decreased, the DNA valves could return to the original state to cap the pores and prevent the cargo from leaking. Hence, the on/off state and release behaviour of the nanocarrier could be controlled precisely by changing the temperature. The details of this strategy are shown in Scheme 1.

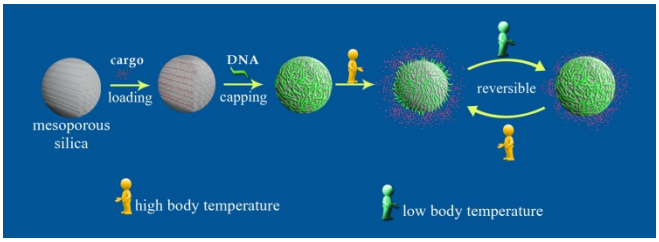

Scheme 1 Schematic illustration of the temperature-responsive nanocarrier for controlled release.

The amino functionalized mesoporous silica support was loaded with rhodamine B (RhB), then the carboxyl modified single-stranded DNA with different length (10-40 bases) were anchored with amino group on the surface of the MSNs acting as the valve (Table S1, ESI†). The critical release temperature of these nanocarriers was assessed by observing the fluorescence changes of RhB as a function

College of Chemistry, Chemical Engineering and Materials Science, Synergetic Innovation Center of Chemical Imaging Functionalized Probes, Key Laboratory of Molecular and Nano Probes, Ministry of Education, Shandong Normal University, Jinan 250014, P.R. China. E-mail: tangb@sdnu.edu.cn

† Electronic Supplementary Information (ESI) available: Experimental details and supporting figures. See DOI: 10.1039/b000000x/

‡ These authors contributed equally to this work.

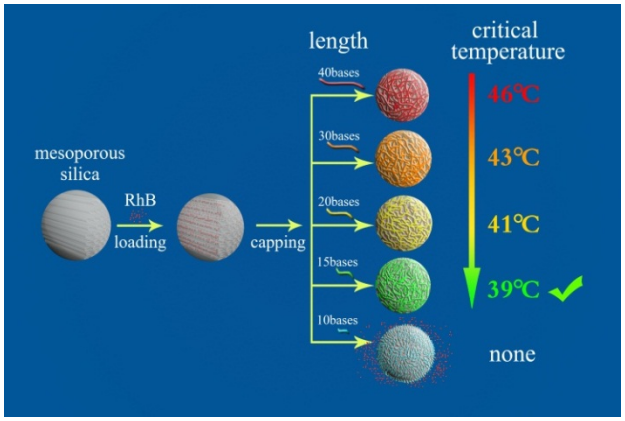

Scheme 2 Scheme of different critical temperature for different DNA valves.

of temperature (Table S2, ESI†). For the nanocarrier with DNA valve of 40 bases, the release amounts of RhB molecules did not show obvious change (<7%) when the temperature was lower than 46 °C (Fig. S1A, ESI†). It demonstrated that the DNA valves were still closed below the current temperature due to the existence of the electrostatic interaction between DNA and the silica. However, the release amounts of RhB molecules was increased (about 75%) within 60 min when the temperature was ≥46 °C. This indicated that the critical temperature of MS-DNA1(RhB) was 46 °C. Once the temperature was above the critical temperature, the electrostatic interaction was destroyed which lead to the valves "on" and the release of cargo molecules. As shown in Fig. S1, the critical temperature (46 °C, 43 °C, 41 °C and 39 °C) of the nanocarriers was decreased with the decrease of the DNA valve length. Nevertheless, the cargo molecules were released continuously at all the setting temperatures and there was no obvious difference in RhB release when the length of DNA valve was decreased to 10 bases, which was similar with the case of MS(RhB) (Fig. S2, ESI†). The reason was that the length of DNA5 was too short to cap the pores of mesoporous silica. In the following experiments, MS-DNA4(RhB) with critical release temperature of 39 °C was chosen as an example, because the critical release temperature should be tuned to a value above the body temperature (37 °C) but below the hyperthermia temperature (42 °C) for intracellular or in vivo applications.[12] The proposed scheme is described in Scheme 2.

Amino-functionalized mesoporous silica nanoparticles (MS-NH_2) were synthesized according to a previously reported method.[13] High resolution transmission electron microscopy (Fig. 1A) showed that the as-prepared MS-NH_2 have an average diameter of about 75 nm and obvious mesopore structure was observed, which offered the opportunity to be used as a general drug carrier. The powder X-ray diffraction (XRD) pattern of MS-NH_2 (Fig. 1C) showed three low-angle reflections typical of a hexagonal array and the clearly observed peaks strongly suggested the three-dimensional mesoporous MCM-41 scaffolding. N_2 adsorption-desorption isotherms were also recorded. The application of the BET model resulted in a value for the total specific surface of 880.77 m^2/g and an average pore diameter calculated using BJH model was about 2.7 nm with a narrow pore-size distribution (Fig. S3, ESI†). The amounts of amino group were determined to be approximately 5.16 μmol/g by TGA analysis (Fig. S4, ESI†), which was the preliminary evidence of the existence of amino group on the MS-NH_2. RhB molecules were then loaded into the mesopores of the MS-NH_2. DNA4 was used as the gatekeeper to cap the pores to prevent the cargo from leaking. The MS-DNA4 was manufactured through the

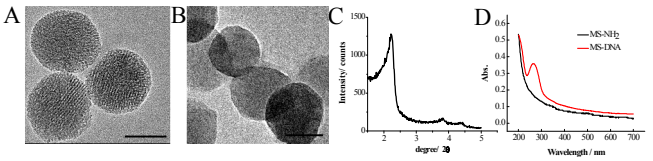

Fig. 1 (A) HRTEM image of MS-NH_2. (B) HRTEM image of MS-DNA4. (C) XRD patterns of MS-NH_2. (D) UV-vis spectra of MS-NH_2, MS-DNA4. Scale bars are 50 nm.

amidation reaction of MS-NH_2 with carboxyl-functionalized DNA4. Fig. 1B showed the morphology of MS-DNA4 did not change obviously after the modification of DNA valves. The UV-vis absorption spectra of MS-NH_2 and MS-DNA4 were shown in Fig. 1D. The appearance of the peak at 260 nm for MS-DNA4 was attributed to the DNA absorbance, indicating the successful modification of DNA4 on the MS-NH_2 surface. Zeta potential experiments further confirmed the successful treatment of the nanocarrier at different stages, i.e., -25.8±0.2mV (MSNs), +57.8±2.2mV (MS-NH_2) and -18.4±1.3mV (MS-DNA4).

Fluorescence analysis was applied to quantify the RhB loaded in the nanocarrier. The fluorescence of the completely released RhB was measured and the concentration of RhB was determined according to a standard linear calibration curve of RhB (Fig. S5, ESI†). The quality of loaded RhB was calculated to be 0.044 mg RhB per 1 mg MS-NH_2. The stability of the nanocarrier was evaluated by time-dependent fluorescence changes at room temperature. Fig. 2A showed that less than 5% RhB escaped from MS-DNA4(RhB) after 60 h, suggesting that the DNA valves could prevent the cargo from leaking effectively. Then the nanocarriers were heated for 90 min in a 39 °C water bath, more than 70% RhB was released, indicating that the DNA valves could open as expected.

The controlled release of the MS-DNA4(RhB) was determined with fluorescence spectroscopic analysis. To evaluate the reversibility and the controlled release behaviour of the nanocarrier, the MS-DNA4(RhB) solutions were manipulated for four high/low temperature cycles. In each cycle, the sample was heated at 39 °C for 15 min and then stopped heating and placed at 37 °C for 12 h in darkness. The fluorescence of the supernate was measured at 15 min and 12 h of each cycle. As shown in Figure 2B, the release amounts of RhB were obviously increased after heating in each cycle, while negligible RhB was released from the nanocarrier during the low temperature stages. The result showed that the cargo molecules could be released upon heating, demonstrating that the DNA valves were open at high temperature. Meanwhile, the release of the cargo molecules was inhibited when the heating was stopped, suggesting that the DNA valves were closed again. It indicated that the nanoca-

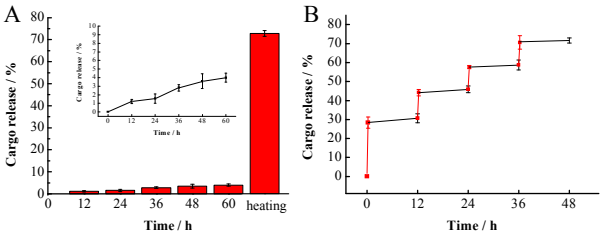

Fig. 2 (A) The leakage of MS-DNA4(RhB) (0.02 mg/mL) over a time profile.Then the sample was heated at 39 °C for 90 min. (B) Controlled release profile of MS-DNA4(RhB) (0.02 mg/mL) for different high/low temperature cycles.

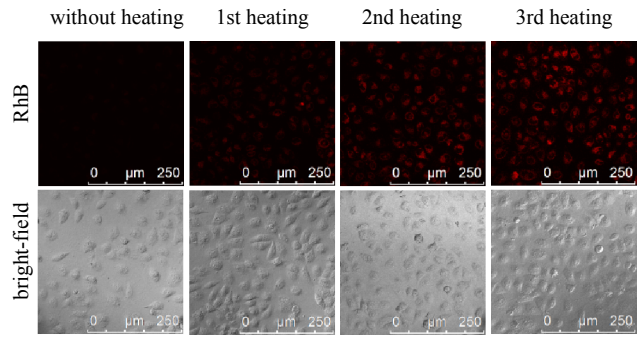

Fig. 3 Confocal fluorescence imaging of MCF-7 cells for different high/low temperature cycles. In each cycle, the cells were first heated at 39 °C for 10 min and then incubated at 37 °C for another 110 min.

rrier was reversible for every high/low temperature cycle.

Before applying the nanocarriers in living cells, the nuclease resistance ability was evaluated under physiological conditions. Enzyme deoxyribonuclease I (DNase I),[14] a common endonuclease, was employed to assess the nuclease stability of the nanocarrier. Fig. S6A showed that the nanocarrier exhibited slight degradation after DNase I was added. When the nanocarrier only and nanocarrier/DNase I solutions were heating in water bath at 39 °C for 90 min, the fluorescence intensity of the two samples increased greatly (Fig. S6B ESI†). The results indicated the nanocarrier possessed high resistance to nuclease and the release of cargo molecules was indeed due to the increased temperature. The nanocarrier could prevent unexpected release of cargo molecules caused by nuclease degradation and it was capable of applying in living cells.

For the application of body temperature triggered nanocarrier for controlled delivery, intracellular release experiment was carried out in a human breast cancer cell line (MCF-7). As shown in Fig. 3, negligible fluorescence signal was observed under confocal laser scanning microscopy when the MCF-7 cells were incubated with MS-DNA4(RhB) at low temperature (37 °C). In order to confirm the controlled release in living cells, three high/low temperature cycles were performed in the same cells. For each cycle, the cells were heating to be 39 °C for 10 min and then incubated at 37 °C for another 110 min. After the first heating, a faint fluorescence signal was observed, indicating the successful release of RhB. The fluorescence signal was gradually enhanced along with the increasing cycles. The average fluorescence intensity of cells after each high temperature process was also measured, which further confirmed the increasing release of the RhB (Fig. S7, ESI†). Next, we performed another confocal imaging experiment as control. The cells with MS-DNA4(RhB) were heated at 39 ^{o}C for 10 min only once and then cultured at 37 ^{o}C for 4 h. As shown in Fig. S8, the fluorescence signals did not show obvious change when the cells were incubated for another 4 h. It indicated that the gradually enhanced fluorescence intensity was indeed caused by the increase of the temperature. The results of flow cytometry of MS-DNA4(Dox) also showed that the fluorescence intensity increased gradually with the increase of the high/low temperature cycles (Fig. S9, ESI†). It demonstrated that the nanocarriers could be triggered by the high body temperature and the controlled delivery could be achieved in living cells.

To evaluate the cytotoxicity of the nanocarrier, an MTT (3-(4, 5-dimethylthiazol-2-yl)-2, 5-diphenyltetrazolium bromide) assay in MCF-7 cells was performed. The absorbance of MTT at 490 nm depends on the degree of activation of the cells. The cell viability was expressed by the ratio of the absorbance of the treated cells (incubated with the nanocarriers) to that of the untreated cells. Fig. S10 showed that the cell viability was more than 97% when the concentration of the nanocarrier was up to 0.08 mg/ml, indicating that the nanocarrier exhibited almost no cytotoxicity or side effects in living cells. Then doxorubicin (Dox) was loaded to investigate if the therapeutic effect could be controlled using the current nanocarrier. The results showed the cell viability decreased with increasing number of high/low temperature cycles (Fig. S11, ESI†).

In conclusion, we have developed a novel temperature-triggered nanocarrier based on mesoporous silica with reversible DNA valves. The reversible DNA valves of the nanocarrier were manipulated by switching the temperature high/low states, which was capable of controlling the release amounts of cargo molecules. The critical temperature for opening valve could be controlled by adjusting the length of DNA valves. An ideal critical release temperature (39 °C) was obtained when 15-base DNA was used as the valve. Moreover, the nanocarrier possesses good stability, high nuclease resistance and good biocompatibility. Intracellular imaging experiment indicated that controlled release could be achieved in living cells. Compared to the reported nanocarriers, the current approach could deliver the cargo molecules accurately in the range of body temperature without any external stimulus. We anticipate that the nanocarrier could provide new opportunities for designing the on-command drug delivery systems.

This work was supported by 973 Program (2013CB933800), National Natural Science Foundation of China (21227005, 21390411, 91313302, 21035003, 21375081, 21105059) and Program for Changjiang Scholars and Innovative Research Team in University.

Notes and references

1 K. Riehemann, S. W. Schneider, T. A. Luger, B. Godin, M. Ferrari, H. Fuchs, *Angew. Chem. Int. Ed.* 2009, **48**, 872; Z. Li, J. C. Barnes, A. Boscoy, J. F. Stoddart, J. I. Zink, *Chem. Soc. Rev.* 2012, **41,** 2590.
2 E. Aznar, M. D. Marcos, R. Martinez-Manez, J. Soto, P. Amoros, C. Guillem, *J. Am. Chem. Soc.* 2009, **131**, 6833; H. P. Rim, K. H. Min, H. J. Lee, S. Y. Jeong, S. C. Lee, *Angew. Chem. Int. Ed.* 2011, **50**, 8853.
3 K. Patel, S. Angelos, W. R. Dichtel, A. Coskun, Y. W. Yang, J. I. Zink, J. F. Stoddart, *J. Am. Chem. Soc.* 2008, **130**, 2382; P. D. Thornton, A. Heise, *J. Am. Chem. Soc.* 2010, **132**, 2024.
4 C. Y. Lai, B. G. Trewyn, D. M. Jeftinija, K. Jeftinija, S. Xu, S. Jeftinija, V. S. Y. Lin, *J. Am. Chem. Soc.* 2003, **125**, 4451; R. Liu, X. Zhao, T. Wu, P. Feng, *J. Am. Chem. Soc.* 2008, **130**, 14418.
5 E. Climent, M. D. Marcos, R. Martínez-Máñez, F. Sancenón, J. Soto, K. Rurack, P. Amorós, *Angew. Chem. Int. Ed.* 2009, **48**, 8519.
6 C. Park, K. Lee, C. Kim, *Angew. Chem. Int. Ed.* 2009, **48**, 1275; J. Croissant, J. I. Zink, *J. Am. Chem. Soc.* 2012, **134**, 7628.
7 C. R. Thomas, D. P. Ferris, J. H. Lee, E. Choi, M. H. Cho, E. S. Kim, J. Cheon, J. I. Zink, *J. Am. Chem. Soc.* 2010, **132**, 10623.
8 S. W. Choi, Y. Zhang, Y. Xia, *Angew. Chem. Int. Ed.* 2010, **122**, 8076.
9 E. Climent, R. Martínez-Máñez, F. Sancenón, M. D. Marcos, J. Soto, A. Maquieira, P. Amorós, *Angew. Chem. Int. Ed.* 2010, **49**, 7281; A. Schlossbauer, S. Warncke, P. M. E. Gramlich, J. Kecht, A. Manetto, T. Carell, T. Bein, *Angew. Chem. Int. Ed.* 2010, **49**, 4734; E. Ruiz-Hernandez, A. Baeza, M. Vallet-Regi, *ACS Nano.* 2011, **5**, 1259; J. Yang, X. Liu, Z. Liu, F. Pu, J. S. Ren, X. G. Qu, *Adv. Mater.* 2012, **24**, 2890; Y. T. Chang, P. Y. Liao, H. S. Sheu, Y. J. Tseng, F. Y. Cheng, C. S. Yeh, *Adv. Mater.* 2012, **24**, 3309.
10 I. I. Slowing, J. L. Vivero-Escoto, C. W. Wu, V. S. Y. Lin, *Adv. Drug Deliv. Rev.* 2008, **60**, 1278; Z. Li, J. C. Barnes, A. Bosoy, J. F. Stoddart, J. I. Zink, *Chem. Soc. Rev.* 2012, **41**, 2590; P. Yang, S. Gai, J. Lin, *Chem. Soc. Rev.* 2012, **41**, 3679.
11 N. Li, Z. Z. Yu, W. Pan, Y. Y. Han, T. T. Zhang, B. Tang, *Adv. Funct. Mater.* 2013, **23**, 2255.

12 L. H. Reddy, J. L. Arias, J. Nicolas, P. Couvreur, *Chem. Rev.* 2012, **112**, 5818; E. Fleigea, M. A. Quadirb, R. Haag, *Adv. Drug Deliv. Rev.* 2012, **64**, 866.
13 J. Kim, H. S. Kim, N. Lee, T. Kim, H. Kim, T. Yu, I. C. Song, W. K. Moon, T. Hyeon, *Angew. Chem. Int. Ed.* 2008, **47**, 8438.
14 D. S. Seferos, A. E. Prigodich, D. A. Giljohann, P. C. Patel, C. A. Mirkin, *Nano Lett.* 2009, **9**, 308; N. Li, C. Chang, W. Pan, B. Tang, *Angew. Chem. Int. Ed.* 2012, **51**, 7426.

